

1
2
3
4
5
6
7
8
9
10
11
12
13
14
15
16
17
18
19
20
21
22
23
24
25
26
27
28

The inattentional rhythm in audition

Troby Ka-Yan Lui*^{1,2}, Eva Boglietti¹, Benedikt Zoefel*^{1,2}

Université de Toulouse III Paul Sabatier, Toulouse, France

Centre National de la Recherche Scientifique (CNRS), Centre de Recherche Cerveau et
Cognition (CerCo), UMR 5549, Toulouse, France

* Corresponding Author: Troby Ka-Yan Lui (trobylui@gmail.com), Benedikt Zoefel
(benedikt.zoefel@cnrs.fr)

Acknowledgements: This study was supported by a grant from the Agence Nationale de la Recherche (ANR-21-CE37-0002). The authors thank Quentin Busson for help with data collection.

29

30

31 **Abstract**

32 The detection of temporally unpredictable visual targets depends on the preceding phase of alpha
33 oscillations (~7-12 Hz). In audition, however, such an effect seemed to be absent. Due to the
34 transient nature of its input, the auditory system might be particularly vulnerable to information
35 loss that occurs if relevant information coincides with the low excitability phase of the
36 oscillation. We therefore hypothesised that effects of oscillatory phase in audition will be
37 restored if auditory events are made task-irrelevant and information loss can be tolerated. To this
38 end, we collected electroencephalography (EEG) data from 29 human participants (21F) while
39 they detected pure tones at one sound frequency and ignored others. Confirming our hypothesis,
40 we found that the neural response to task-irrelevant but not to task-relevant tones depends on the
41 pre-stimulus phase of neural oscillations. Alpha oscillations modulated early stages of stimulus
42 processing, whereas theta oscillations (~3-7 Hz) affected later components, possibly related to
43 distractor inhibition. We also found evidence that alpha oscillations alternate between sound
44 frequencies during divided attention. Together, our results suggest that the efficacy of auditory
45 oscillations depends on the context they operate in, and demonstrate how they can be employed
46 in a system that heavily relies on information unfolding over time.

47

48 **Significance Statement**

49 The phase of neural oscillations shapes visual processing, but such an effect seemed absent in the
50 auditory system when confronted with temporally unpredictable events. We here provide
51 evidence that oscillatory mechanisms in audition critically depend on the degree of possible
52 information loss during the oscillation's low excitability phase, possibly reflecting a mechanism
53 to cope with the rapid sensory dynamics that audition is normally exposed to. We reach this
54 conclusion by demonstrating that the processing of task-irrelevant but not task-relevant tones
55 depends on the pre-stimulus phase of neural oscillations during selective attention. During
56 divided attention, cycles of alpha oscillations seemed to alternate between possible acoustic
57 targets similar to what was observed in vision, suggesting an attentional process that generalises
58 across modalities.

59

60

61

Introduction

62 Confronted with a dynamic environment, our brain constantly engages in the selection and
63 prioritization of incoming sensory information. Previous research posits that neural oscillations,
64 rhythmic fluctuations in neural excitability, are instrumental for this purpose (Schroeder &
65 Lakatos, 2009). One fundamental assumption in this line of research is that the sensory
66 information that coincides with the high-excitability phase of an oscillation is processed more
67 readily than that occurring during the low-excitability phase, leading to perceptual or attentional
68 rhythms (VanRullen, 2016b).

69 Previous studies in the visual modality have confirmed this assumption, demonstrating
70 that the detection of temporally unpredictable targets depends on the pre-stimulus phase of alpha
71 oscillations in the EEG (Busch et al., 2009; Dugué et al., 2015; Dugué et al., 2011; Mathewson et
72 al., 2009). This phasic effect was only found for the detection of attended, but not unattended
73 visual targets (Busch & VanRullen, 2010).

74 Studies in the auditory modality, however, revealed a more ambivalent role of neural
75 oscillations in auditory perception (VanRullen et al., 2014). On the one hand, the detection of
76 near-threshold auditory tones, presented at unpredictable moments in quiet, does not depend on
77 pre-target neural phase (VanRullen et al., 2014; Zoefel & Heil, 2013). This result seems to
78 question the assumption of an auditory perception that is inherently rhythmic. On the other hand,
79 it is clear that stimulus-aligned (“entrained”) neural oscillations serve a mechanistic role in
80 auditory attention and perception (Obleser & Kayser, 2019; Henry & Obleser, 2012; van Bree et
81 al., 2021). Rhythmicity in auditory processing can also be observed after a cue like the onset of
82 acoustic noise, assumed to reflect a phase reset of oscillations in the theta range (Ho et al., 2017;
83 Lui et al., 2023; Wöstmann et al., 2020).

84 We here tested a hypothesis that can reconcile these apparently discrepant findings. This
85 hypothesis is based on the fact that the auditory environment is particularly dynamic and
86 transient (Kubovy, 1988; VanRullen et al., 2014). Losing critical auditory information that
87 coincides with the low-excitability phase of the oscillation may be too costly for successful
88 comprehension of auditory input. To avoid such a loss of information, the brain may therefore
89 suppress neural oscillations in auditory system and operate in a more “continuous mode”
90 (Schroeder & Lakatos, 2009) if incoming auditory stimuli are relevant (e.g., attended) but their
91 timing is unknown. This assumption predicts two scenarios in which a “rhythmic mode” can be
92 restored (Zoefel & VanRullen, 2017). First, if the timing of relevant events is known, the phase
93 of the oscillation can be adapted accordingly, and a loss of critical information during the low-
94 excitability phase avoided. As explained above, such an effect is fundamental for the field of
95 “neural entrainment” (Lakatos et al., 2008, 2019). A second scenario remained unexplored and
96 was tested here: The temporary suppression of input processing during the low-excitability phase
97 can be tolerated if expected events are irrelevant to perform a task, even if their timing is
98 unpredictable. In this scenario, the processing of irrelevant (but not relevant) events would be
99 modulated by the oscillatory phase.

100 We measured participants' EEG and asked them to detect pure tones at one sound
101 frequency (task-relevant tone) and ignore pure tones at another sound frequency (task-irrelevant
102 tone), presented at unpredictable moments (Figure 1A). We predicted that the processing of the
103 task-irrelevant, but not that of the task-relevant tone, depends on the phase of neural oscillations.
104 In a condition where both tones needed to be detected, we tested whether the presence of
105 multiple task-relevant tones leads to a rhythmic alternation of attentional focus between these
106 tones – and consequently, a phasic modulation of detection even for task-relevant tones – as
107 previously demonstrated for the visual system (Fiebelkorn et al., 2013; Helfrich et al., 2018).

108

109

110

Materials and Methods

111 Participants

112 Thirty native French participants took part in the experiment with informed consent for a
113 monetary reward of €25. The data of one participant was excluded due to technical issues, thus
114 29 participants (21 females, mean age = 22.34, SD = 1.2) were included in the final data
115 analyses. All experimental procedures were approved by the CPP (Comité de Protection des
116 Personnes) Ouest II Angers (protocol number 21.01.22.71950 / 2021-A00131-40).

117

118 Experimental Design

119 Participants performed a tone-in-noise detection task where they were presented with pure tones
120 at two different sound frequencies (440 Hz and 1026 Hz), embedded at unpredictable moments
121 into a continuous stream of pink noise (Figure 1A). They were instructed to press a button when
122 they hear a tone at the to-be-attended, task-relevant sound frequency and ignore the other one. A
123 correct detection was defined as a button press within 1 second after pure tone onset throughout
124 the experiment. All tones were 20ms in duration with a rise-and-fall period of 5ms. The
125 continuous pink noise was presented at ~70 dB SPL. Prior to the main experiment, the sound
126 level of the pure tones was titrated individually so that ~50% of tones were detected in the main
127 task (see Adaptive Staircase Procedure). In total, 504 pure tones at each sound frequency were
128 presented. These were divided into 12 experimental blocks, each ~ 5 min long.

129 In “selective attention” blocks, participants had to detect tones at one of the two sound
130 frequencies and to ignore the other. In “divided attention” blocks, they had to detect tones at both
131 sound frequencies. The order of the tones was pseudo-randomized with the constraint of a
132 transitional probability between 0.24 and 0.26. The stimulus-onset asynchrony between tones
133 was randomized between 2 and 5s with a uniform distribution to ensure temporal
134 unpredictability. The unpredictability of the tones prevented potential preparatory responses to
135 the upcoming stimulus. We adopted a rolling adaptive procedure to ensure that participants
136 would detect the tone at threshold level (50%) throughout the experiment. After each block, if
137 the participant’s detection probability was lower than 40% or higher than 60 %, the sound level
138 of the tone at the corresponding pitch was increased or decreased by 1dB, respectively. The
139 block order (selective attention – low pitch, selective attention – high pitch, divided attention)
140 was counterbalanced between participants.

141 Stimulus presentation was done via Matlab 2019a (MathWorks, Inc., Natick, USA) and
142 Psychtoolbox (Brainard, 1997). The auditory stimuli were presented using Etymotic ER-2
143 inserted earphones and a Fireface UCX soundcard. The same sound card was used to send
144 triggers to the EEG system, ensuring synchronisation between sound and EEG.

145

146 **Adaptive Staircase Procedure**

147 Individual detection thresholds were determined separately for each of the two pure tones with a
148 1-up-1-down adaptive staircase procedure as implemented in the Palamedes toolbox (Prins &
149 Kingdom, 2018). In each adaptive trial, one pure tone was embedded randomly between 0.5 and
150 4.5s after the onset of a 5-second pink noise snippet. The participant had to press a button as
151 soon as they detected the pure tone. With a starting value of -30 dB of the total soundcard output
152 (i.e., around 70 dB SPL), the sound level of the tone decreased in steps of 1 dB if the participant
153 correctly detected it, or increased accordingly if they missed the pure tone. The adaptive
154 procedure ended after 10 reversals, and the final 6 reversals were used to calculate the threshold.
155 The convergence of the staircase procedure was examined by visual inspection to determine
156 whether the threshold would be used in the following main experiment. If convergence failed,
157 the adaptive procedure was repeated. The average thresholds for high- and low frequency tones
158 were -39.67 dB (SD = 1.21 dB) and -37.10 dB (SD = 1.26 dB), respectively, resulting in ~ 50%
159 detected tones during both selective and divided attention (Figure 1B).

160

161 **EEG Recording and Data Processing**

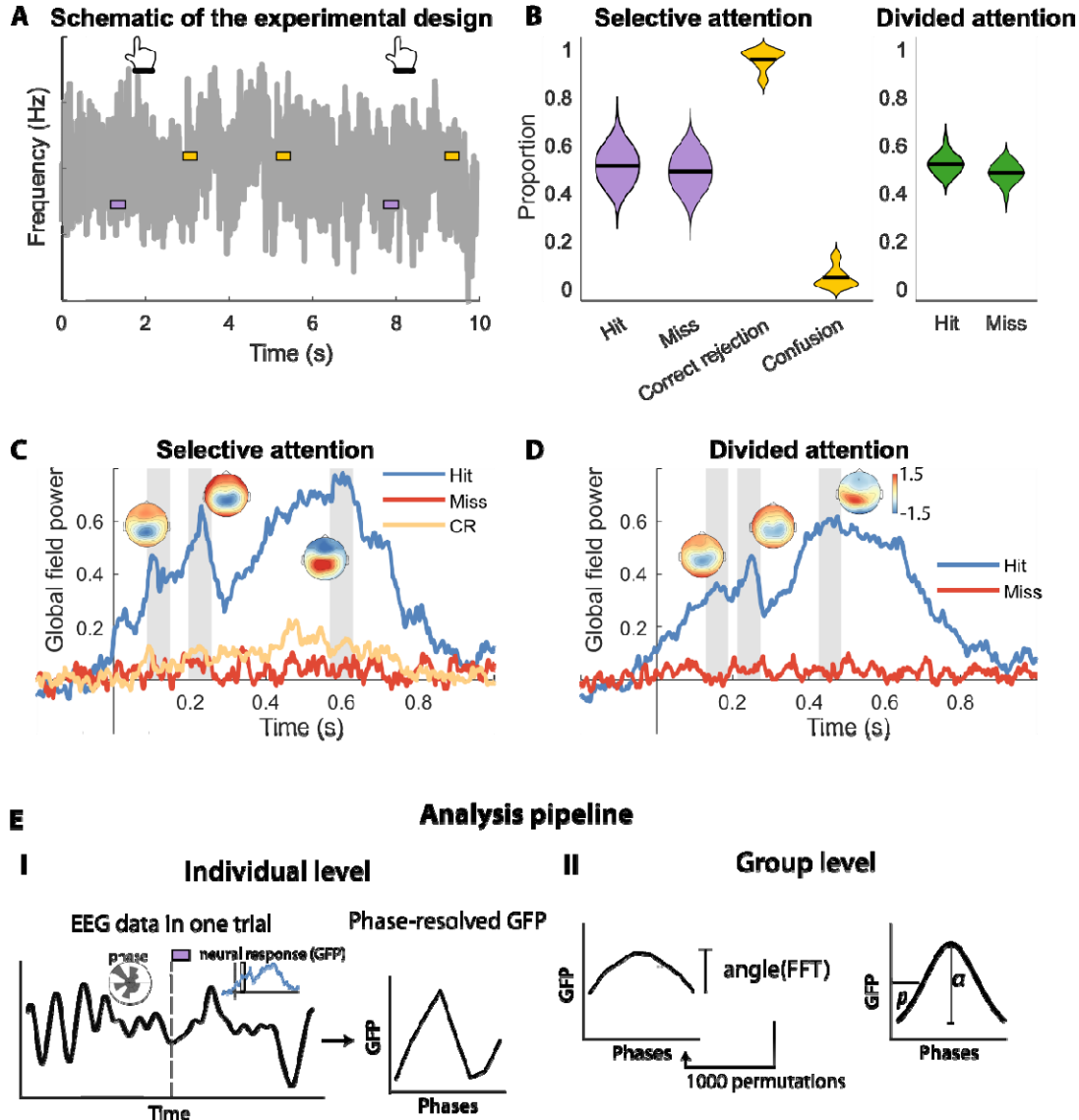
162 EEG was recorded using a Biosemi Active 2 amplifier (Biosemi, Amsterdam, Netherlands). 64
163 active electrodes positioned according to the international 10-10 system. The sampling rate of the
164 EEG recording was 2048 Hz. Equivalent to typical reference and ground electrodes, the Biosemi
165 system employs a “Common Mode Sense” active electrode and a “Driven Right Leg” passive
166 electrode located in the central-parietal region for common mode rejection purposes. The signal
167 offsets of all electrodes were kept under 50 μ V.

168 All EEG pre-processing steps were conducted using Matlab 2021a (MathWorks, Inc.,
169 Natick, USA) and the fieldtrip toolbox (Oostenveld et al., 2011). EEG data were re-referenced to
170 the average of all electrodes. Then, the data were high- and low-pass filtered (4th order
171 Butterworth filter, cut-off frequencies 0.5 Hz and 100 Hz, respectively). Noisy EEG channels
172 were identified by visually inspection and interpolated. Artefacts such as eye blinks, eye
173 movements, muscle movements, and channel noise were detected in an independent component
174 analysis (ICA) applied to down-sampled EEG data with a sampling rate of 256 Hz.
175 Contaminated components were detected by visual inspection and removed from data at the
176 original sampling rate. The continuous EEG data were segmented from -2s to +2s relative to
177 each tone onset, termed “trials” in the following. Trials with an absolute amplitude that exceeded
178 160 μ V were rejected.

179 We did not measure participants’ subjective perception of task-irrelevant tones as this
180 would have rendered them relevant. Instead, we used a neural proxy to infer how readily these
181 tones were processed, and how processing depended on pre-stimulus phase. In line with previous
182 work (Busch & VanRullen, 2010), we used global field power (GFP) evoked by tones as such a
183 proxy. For this purpose, event-related potentials (ERPs) were calculated for each participant,
184 separately for correctly detected (hits) and missed targets (misses) and for each condition in the 2
185 x 2 design (task-relevant vs task-irrelevant, selective vs divided attention). For the selective

186 attention condition, ERPs for trials where participants correctly did not respond to the task-
187 irrelevant tone (correct rejection; CR) were also calculated. GFP was extracted as the low-pass
188 filtered (cut-off frequency 10 Hz) standard deviation of the ERPs across EEG channels. Three
189 relevant time lags for tone processing were determined as local maxima (i.e. peaks identified
190 with the “findpeaks” Matlab function) in the grand average GFP from 0 to 1s after tone onset,
191 separately for selective and divided conditions (Figure 1C). As the aim of this step is the
192 identification of relevant time lags for tone processing, we restricted the analysis to detected
193 task-relevant tones (Figure 1C, D). Time windows of interest for the analysis of phasic effects
194 (see below) were selected as +/- 30ms around each of these three peaks. Single-trial GFP
195 amplitudes were obtained by averaging the GFP amplitude across time points within each time
196 window of interest. This was done separately for each experimental condition, including those
197 without a behavioural response (i.e. the task-irrelevant conditions).

198 We used a fast Fourier transform (FFT) with hanning tapers and sliding windows (0.02 s
199 steps) to extract EEG phases at frequencies from 2 Hz to 20 Hz (1 Hz steps) from single trials
200 and channels. The window size for phase estimation was linearly spaced between 2 (for 2 Hz)
201 and 5.6 (for 20 Hz) cycles of the corresponding frequency. The subsequent analytical steps were
202 restricted to phases estimated from windows that do not include post-stimulus EEG data (cf.
203 Figure 2A). This avoid a potential contamination with stimulus-evoked responses that can lead to
204 spurious phase effects (Vinao-Carl et al., 2024; Zoefel & Heil, 2013).



205

206 *Figure 1.* A) Schematic of the tone-in-noise detection task. Purple and yellow rectangles denote task-relevant and
 207 task-irrelevant tones, respectively. In the main experiment, low and high tones served as task-relevant and task-
 208 irrelevant tones in different blocks. Grey line shows the continuous pink noise. B) Behavioural performance for
 209 selective attention (left) and divided attention (right) conditions. Black lines show the mean across participants. C,D)
 210 Global field power (GFP) for hit (blue; relevant tones), miss (red; relevant tones), and correct rejection (CR; yellow;
 211 irrelevant tones) in the selective (C) and divided (D) attention conditions. Grey areas indicate the time window
 212 selected for the phase dependence analysis. Insets show topographies of GFP at each time window for hit trials. E) Illustration of the analysis pipeline for the phase-dependence analysis. E-I) Extraction of single-trial phase estimates
 213 for individual participants. GFP in each phase bin was calculated to create the phase-resolved GFP values. E-II) The
 214 analysis procedure on the group level with simulated individual phase-resolved GFP for illustration (thin grey lines).
 215 The hypothesized phase effect was quantified by fitting a sine function to the averaged data (bold black line) and
 216 contrasting the amplitude a of this fit against that obtained in a permutation distribution ($N = 1000$). This analysis
 217 assumes that the phase p of individual sine functions is consistent across participants, an assumption that we
 218 verified statistically (see Materials and Method; Results).
 219

220 **Statistical analysis**

221 To address our main hypothesis, we tested whether the magnitude of the stimulus-evoked
222 response (as GFP; see previous section) varies with pre-stimulus neural phase (Figure 1E). We
223 used a statistical approach that a previous simulation study (Zoefel et al., 2019) showed to be
224 particularly sensitive to such phasic effects (“sine fit binned” method in that study). For each
225 condition, participant, EEG channel, frequency and time point separately, single trials were
226 divided into 8 equally spaced bins according to their phase (Figure 1E-I) and the average GFP
227 amplitude extracted for each phase bin. We then fitted a sine function to the resulting phase-
228 resolved GFP amplitude (Figure 1E-II). The amplitude of this sine function (a in Figure 1E-II)
229 indexes how strongly tone processing is modulated by EEG phase whereas its phase (p in Figure
230 1E-II) reflects “preferred” and “non-preferred” phases for GFP (leading to highest and lowest
231 GFP, respectively). To quantify phase effects statistically, we compared sine fit amplitudes with
232 those obtained in a simulated null distribution, i.e. in the absence of a phasic modulation of tone
233 processing. This null distribution was obtained by randomly assigning EEG phases to single
234 trials and recomputing the amplitude of the sine 1000 times for each condition, EEG channel,
235 frequency and time point (VanRullen, 2016a). For each combination of these factors, the sine
236 amplitude from the original data was compared with the null distribution to obtain group-level z-
237 scores:

238
$$z = (a - \mu) / \sigma$$

239 where z reflects the group level effect in the original data, a is the amplitude value in the original
240 data, and μ and σ are mean and standard deviation (across permutations) of the subject-averaged
241 amplitude in the surrogate distribution, respectively. Z-scores were then converted to p-values
242 (e.g., $z = 1.645$ would corresponds to a significance threshold of $\alpha = 0.05$, one-tailed) and
243 corrected for multiple comparisons using the false discovery rate (FDR). Finally, clusters in
244 combinations of frequency, time, and EEG channel for the FDR-corrected p-values were
245 identified using the “findcluster” function in the fieldtrip toolbox.

246 One advantage of the statistical method used is that it makes explicit assumptions on
247 whether participants have consistent “preferred” EEG phases, reflected in the phase of the sine
248 fitted to individual participants (Figure 1E-II). If these phases are uniformly distributed (i.e.
249 inconsistent across participants), the sine fit amplitude is extracted separately for each participant
250 and then averaged before the comparison with the surrogate distribution. In this way, the z-score
251 defined above is independent of individual preferred EEG phases. If phases are non-uniformly
252 distributed (i.e. consistent across participants), the phase-resolved GFP (Figure 1E-I) is first
253 averaged across participants and the sine function is fitted to the resulting average (Figure 1E-II)
254 before the comparison with the surrogate distribution. In this way, the z-score is only high when
255 its phase is consistent across participants. To test which version of the test is appropriate in our
256 case, we applied a Rayleigh’s test for circular uniformity (Circular Statistics Toolbox; Berens,
257 2009) to the distribution of individual preferred EEG phases at each time-frequency point. We
258 found a pre-stimulus cluster of significant phase consistency across participants (cf. Results), and
259 adapted our statistical method accordingly (using the second version described).

260 We adapted this statistical approach to test whether task-relevant and task-irrelevant tones differ
261 in their phasic modulation. In this version, we contrasted the difference in averaged sine fit
262 amplitudes between the two conditions (relevant vs irrelevant) with another surrogate
263 distribution for which the condition label was randomly assigned to trials. This procedure yielded
264 another z-score which was calculated as described above.

265 In the divided attention condition, we additionally tested whether the processing of the
266 low and high frequency tone has a different preferred phase by comparing the phase difference
267 between the two tone conditions against zero (circular one-sample test against angle of 0;
268 circ_mtest.m in the Circular Statistics Toolbox).

269

270 **Source localisation of the phase-dependence effect**

271 We also explored the neural origins of the effects found in the analysis of EEG phase effects,
272 using standard procedures implemented in the fieldtrip toolbox. For this purpose, we used a
273 standard volume conduction model and electrode locations to calculate the leadfield matrix (10-
274 mm resolution). Then, for the selective attention condition, we calculated a spatial common filter
275 using the LCMV beamformer method (lambda = 5%; Van Veen et al., 1997) on the 20-Hz low-
276 pass filtered EEG data from -1s to -0.5s relative to tone onset. The chosen time window
277 encompasses all of the observed phase effects (cf. Results). This resulted in 2,015 source
278 locations that were inside the brain.

279 Single-trial EEG data from individual participants were projected onto the source space
280 with the spatial common filter. The analysis of phasic effects was then applied to data from each
281 source location as described above for the sensor level. Due to the large computational demand,
282 we used 100 permutations for the construction of surrogate distributions (z-score defined above),
283 a number shown to be sufficient in the past (VanRullen, 2016a). The voxels with the 1% largest
284 z-scores were selected as the origin of the corresponding effects on the sensory level. Note that,
285 due to the low spatial resolution of EEG, we explicitly treat these source-level results as
286 explorative.

287

Results

288 **Overview**

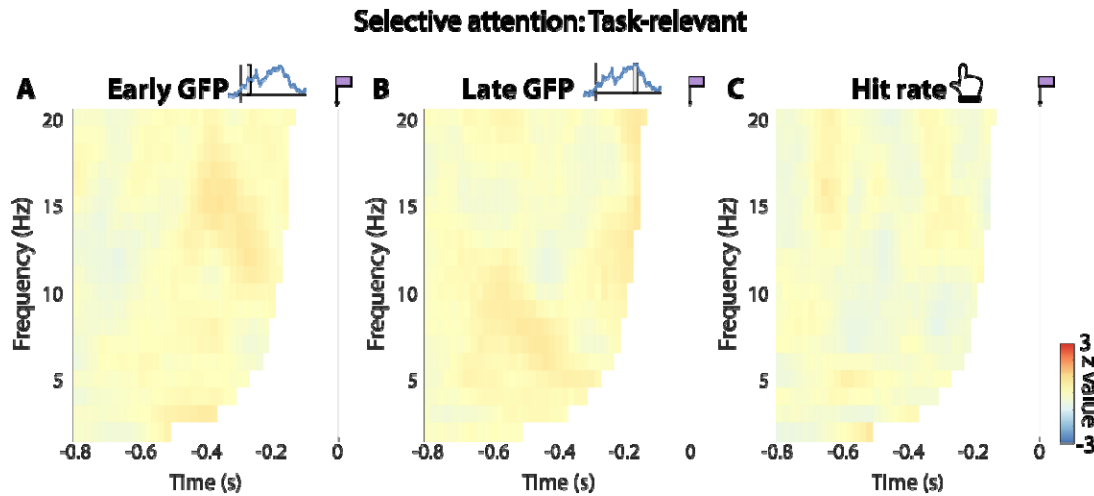
289 Participants were presented with tones at two different sound frequencies (Figure 1A). In some
290 experimental blocks, they were asked to detect one of them (task-relevant tone in the selective
291 attention condition) and ignore the other (task-irrelevant tone in the selective attention
292 condition). In other blocks, they were asked to detect both of them (divided attention condition).

293 On average, participants detected 51.18% (SD = 0.07%) and 51.84% (SD = 0.04%) of
294 task-relevant tones during selective and divided attention, respectively (Figure 1B),
295 demonstrating successful titration of individual thresholds (see Materials and Methods).

296 During both attentional conditions, task-relevant tones produced a strong increase in
297 global field power (GFP) if they were detected but not if they were missed (Figure 1C, D). We
298 therefore used the grand-average evoked GFP as a proxy for tone processing, and identified three
299 time lags with local GFP maxima for further analyses (grey in Figure 1C, D). The time lags for
300 “early”, “medium” and “late” evoked GFP were 119 ms, 227 ms and 598 ms for the selective
301 attention condition, and 159 ms, 243 ms, and 457 ms for the divided attention condition,
302 respectively. We used GFP as a principal measure of tone processing due to the lack of
303 behavioural response to task-irrelevant tones which would otherwise have rendered them
304 relevant. Validating this measure of neural processing, the GFP at each of the three time lags was
305 significantly larger for detected than for missed task-relevant tones during both selective (early:
306 $t_{28} = 7.81, p < .001$; medium: $t_{28} = 7.89, p < .001$; late: $t_{28} = 10.67, p < .001$) and divided attention
307 (early: $t_{28} = 7.46, p < .001$; medium: $t_{28} = 7.22, p < .001$; late: $t_{28} = 8.44, p < .001$).

308 Having identified critical time lags of tone processing, we extracted the GFP at each of
309 the three lags evoked by single tones (including task-irrelevant ones) and tested how strongly
310 GFP depends on pre-stimulus EEG phase in the different conditions (task-relevant vs irrelevant,
311 selective vs divided attention). Following previous work (Lui et al., 2023; Zoefel et al., 2019),
312 we fitted a sine function to GFP as a function of EEG phase (Figure 1E), and used the amplitude
313 of this fit (a in Figure 1E-II) as a measure of phasic modulation strength. Statistical reliability of
314 the phase effects was tested by comparison with a simulated null distribution (as z-score; see
315 Material and Methods).

316 In the following, we illustrate results separately for task-relevant (Figure 2) and task-irrelevant
317 tones (Figure 3) in the selective attention condition, respectively, as well as for the divided
318 attention condition (Figure 4). We only display results for early and late GFP, as no phasic
319 modulation was found for the medium time lag in any of the conditions.



320

321 *Figure 2. Results for task-relevant tones in the selective attention condition. The colour shows how strongly GFP*
322 (*A,B*) and hit rate (*C*) depends on EEG phase, expressed relative to a surrogate distribution, and averaged across
323 channels. Time 0 corresponds to tone onset. In *A* and *B*, insets show relevant time lags for the analysis (early GFP:
324 +119ms ; late GFP: +598ms. Time-frequency points “contaminated” by post-stimulus data (which is “smeared” into
325 pre-stimulus phase estimates during spectral analysis) are masked.

326 **Neural response evoked by task-irrelevant but not task-relevant tones depends on phase of**
327 **neural oscillations during selective attention**

328 We found that pre-stimulus EEG phase did not predict GFP evoked by task-relevant tones at any
329 of the three time lags (all $p > 0.05$ after FDR correction; Figure 2A,B). Consistent with this
330 result, the probability of detecting these tones was independent of pre-stimulus phase (all $p >$
331 0.05 after FDR correction; Figure 2C). In contrast, both early (Figure 3A-C) and late (Figure 3D-
332 F) GFP evoked by task-irrelevant tones depended on pre-stimulus phase.

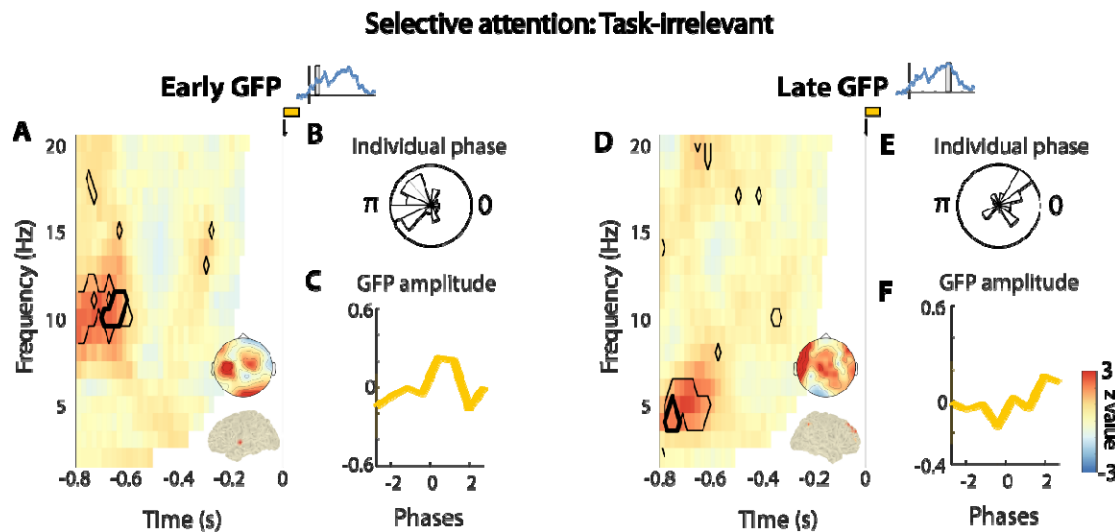
333 For the early lag, the phasic modulation was maximal at 10 Hz and 0.8 s preceding tone onset (z
334 = 5.41, FDR-corrected $p = .003$). The EEG phase leading to maximal GFP at that time-frequency
335 point was consistent across participants (Rayleigh’s test; $z = 6.21$, FDR corrected $p = .006$;
336 Figure 3B). The largest cluster of significant z-scores (FDR-corrected $p < 0.05$) was identified at
337 ~10-11 Hz, in the left central channels, and between -0.7s and -0.62s relative to tone onset
338 (summed $z = 63.2$, 14 time-frequency-channel points; Figure 3A). Explorative source
339 localisation revealed that the phasic modulation originated from the left superior temporal cortex
340 (Figure 3A, inset).

341 For the late lag, the phasic modulation was maximal at 5 Hz and 0.7 s preceding tone
342 onset ($z = 5.49$, FDR-corrected $p = .001$). The EEG phase leading to maximal GFP at that time-
343 frequency point was also consistent across participants ($z = 6.24$, FDR corrected $p = .006$; Figure
344 3E). The largest cluster of significant z-scores was identified at ~4-5 Hz and between -0.78 and -
345 0.74s relative to tone onset (summed $z = 47.45$, 11 time-frequency-channel points; Figure 3D).
346 This effect was localised to the right superior frontal gyrus and, to a lesser extent, the right
347 inferior parietal cortex (Figure 3D, inset).

348

349 Contrasting amplitudes of the fitted sine functions between task-relevant and task-
350 irrelevant tones, we found a stronger phasic modulation for the task-irrelevant tones at their
351 relevant time-frequency points (Figure 3A,D) that concerned both early GFP ($z = 4.08, p < .001$;
352 paired t-test) and late GFP ($z = 2.92, p = .004$). However, neither of these outcomes survived
353 correction for multiple comparison ($p > 0.05$ after FDR correction).

354 Together, our results confirm previous findings that the processing of task-relevant
355 auditory information is independent of the phase of neural oscillations (Zoefel & Heil, 2013),
356 and extend them by demonstrating that such a phasic modulation reappears when the information
357 is made irrelevant. Both alpha and theta oscillations, through their correspondence with different
358 stages of neural processing, seem to contribute to rhythmic effects on unattended information
359 during selective attention.



360

361 *Figure 3. Results for task-irrelevant tones in the selective attention condition. A, D) Same as Figure 2A,B, but for*
362 *task-irrelevant tones, and for channels selected for their significant phasic modulation of GFP ($p < .05$ after FDR*
363 *correction). Black contours show the time-frequency points with significant phase effects. Bold black contours show*
364 *the cluster with the largest summed z-score. Upper insets on the two panels show the topographical maps of z-scores*
365 *in the corresponding time-frequency clusters. Lower insets show the 1% voxels with the largest source-projected z-*
366 *scores in the same clusters. B, E) Distribution of individual phases of the sine function fitted to phase-resolved GFP*
367 *(p in Figure 1E-II), at the time-frequency-channel combination with strongest phasic modulation (B: 11 Hz, -0.64s,*
368 *C5; E: 4 Hz, -0.76s, FT7). C, F) GFP as a function of EEG phase from the same time-frequency-channel*
369 *combination. The bold line shows the group-level average, the shaded area shows its standard error. Insets next to*
370 *the titles show the GFP from Figure 1C with the time windows at which the analysis was performed.*

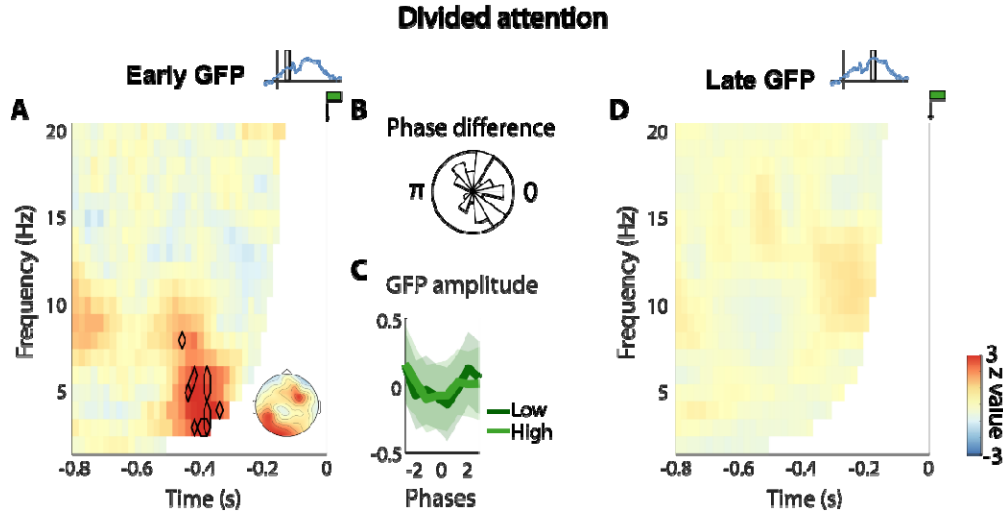
371

372 **Early but not late response evoked by task-relevant tones depends on phase of neural**
373 **oscillations during divided attention**

374 In the divided attention condition, only task-relevant tones were present. According to our
375 principal hypothesis, the auditory system should suppress oscillations and instead operate in a
376 continuous mode of processing to avoid a loss of information at the low-excitability phase.
377 However, an alternative possibility is that the presence of multiple target tones requires a
378 rhythmic alternation of attentional focus between these tones as previously demonstrated for the
379 visual system (Fiebelkorn et al., 2013; Helfrich et al., 2018). Such a case would lead to a phasic
380 modulation of tone processing, similarly to what we observed for task-irrelevant tones in the
381 selective attention condition.

382 Figure 4 shows how strongly the evoked GFP at early (A) and late (D) time lags depended on
383 pre-stimulus EEG phase in the divided attention condition. We found a phasic modulation of
384 tone processing only for the early time lag. This effect was maximal at 3 Hz and 0.42 s preceding
385 tone onset ($z = 5.09$, FDR-corrected $p = .01$). However, we could not identify a cluster of
386 significant z-scores, suggesting that these did not conglomerate in neighbouring electrodes,
387 frequency, or time as evidently as for the selective attention condition. EEG phase leading to the
388 strongest early GFP were similar for low- and high-frequency tones (Figure 4C), supported
389 statistically by a distribution of their phase difference (Figure 4B) that did not significantly differ
390 from zero (mean angle = 0.23, $p = .71$; circular one-sample test against angle of 0). The
391 probability of detecting tones did not depend on pre-stimulus phase during divided attention (all
392 FDR corrected $p < 0.05$; results for time-frequency point with strongest effect in Figure 4A: $z =$
393 0.89, $p = 0.37$).

394 Together, our results show that a rhythmic mode of processing reappears in the auditory system
395 when confronted with multiple targets, but only affects early stages of target processing. In the
396 presence of two target tones, the frequency of modulation is approximately divided by half as
397 compared to a single tone, and the two target tones have similar preferred EEG phases for their
398 processing. These results speak for a mechanism processing each of the two tones at subsecutive
399 cycles of a faster rhythm, as we explain in the Discussion.



400

401 *Figure 4. Results for task-relevant tones in the divided attention condition. All conventions as in Figure 3, apart*
402 *from panel B, which illustrates the distribution of phase difference between low- and high-frequency tones, and*
403 *panel C, where results are shown separately for the low- and high frequency tones.*

404

Discussion

405 The current study aimed to unveil the rhythm of auditory perception during selective and divided
406 attention. To this end, we asked participants to perform a target-in-noise detection task where
407 they had to attend to tones at one sound frequency and ignore another (selective attention), or
408 had to attend to both (divided attention).

409 In line with previous work (Zoefel & Heil, 2013; VanRullen et al., 2014) and our own
410 hypothesis, we found that neural and behavioural responses to task-relevant tones do not depend
411 on the pre-stimulus phase of neural oscillations during selective attention. Conversely, early and
412 late neural responses to task-irrelevant tones were modulated by the phase of pre-stimulus alpha
413 and theta oscillations, respectively. These results demonstrate that while neural oscillations seem
414 to be suppressed during attentive selection of single auditory targets, there exists a rhythmic
415 mode of perception in the auditory system that is applied to unattended sensory information.
416 Finally, we found evidence that this mode is also active when confronted with multiple auditory
417 targets, although restricted to early stages of their processing.

418

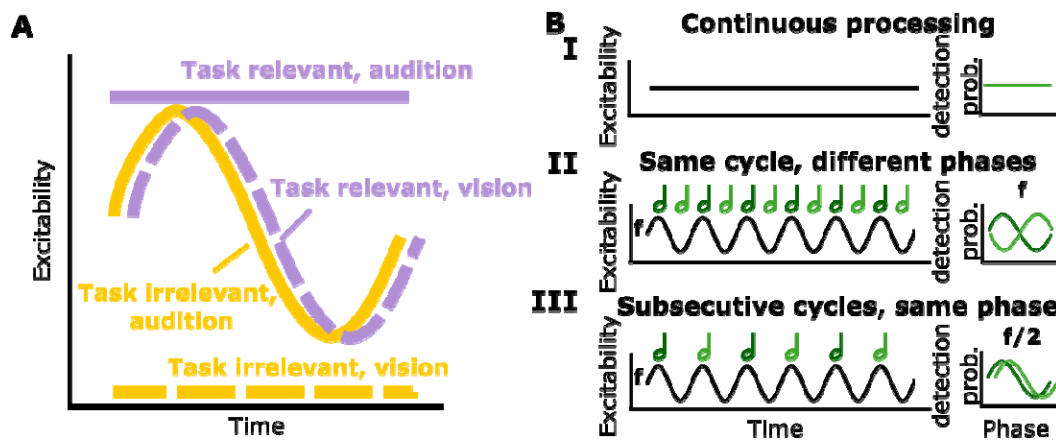
419 An inattentional rhythm in audition

420 It is a striking difference between modalities that selective attention *increases* the effect of neural
421 phase on the processing of temporarily unpredictable targets in the visual domain (Busch &
422 VanRullen, 2010) but *decreases* it in the auditory one (Zoefel & Heil, 2013; current study).
423 Confirming previous speculations (Zoefel & VanRullen, 2017), we here demonstrate that a
424 rhythmic mode of auditory processing is restored when stimuli become irrelevant and
425 information loss is tolerable. This “inattentional rhythm” that seems specific to audition may
426 arise from specific requirements on the auditory system during dynamic stimulus processing.

427 In contrast to the relatively stable visual environment, auditory inputs are often transient
428 and dynamic. Therefore, periodic sampling of the external environment may be more detrimental
429 for audition when temporarily unpredictable information is important for goal-directed
430 behaviour. In this case, the auditory system may engage in a desynchronised cortical state in the
431 auditory cortex that is associated with the active processing of incoming sensory inputs
432 (Pachitariu et al., 2015). As much as this “continuous mode” prevents the loss of information by
433 suppressing periodic moments of low excitability, it is likely to be metabolically demanding
434 (Schroeder & Lakatos, 2009). Therefore, the auditory system may limit the use of such a mode to
435 scenarios in which a loss of information is likely (such as the expectation of relevant events
436 whose timing cannot be predicted). This notion can also explain the prevalence of rhythm in
437 acoustic information (music, speech etc.): If relevant events are presented regularly, then their
438 timing can be predicted and the oscillatory phase adapted accordingly (Lakatos et al., 2008).
439 Such a mechanism would enable a “rhythmic mode” of processing even for task-relevant stimuli.

440 Based on these results, we propose that – due to its highly dynamic environment – the auditory
441 system always needs to be “one degree more attentive” to sensory information than the visual
442 one. We illustrate this idea in Figure 5A that can be summarised as follows: In the presence of

443 temporarily unpredictable, relevant information, the auditory system needs to operate in a
444 continuous mode of high-excitability, whereas the visual system can sample rhythmically, due to
445 the significantly slower input dynamics. A similar rhythmic mode of processing is used in the
446 auditory system to sample unattended input, whereas it is processed in a mode of continuous low
447 sensitivity in the visual case. The latter explains why we observed a phasic modulation of task-
448 irrelevant tones in the current study, in contrast to an absence of such an effect in the visual
449 modality (Busch & VanRullen, 2010). Our model is also supported by the finding that auditory
450 distractors are more distracting than visual distractors (Berti & Schröger, 2001), even when the
451 primary task is in the visual modality (Lui & Wöstmann, 2022). This might be because the
452 auditory system exhibits periodic moments of high sensitivity to distractors and is therefore also
453 more sensitive to potentially threatening stimuli that warrant immediate action.



454
455 *Figure 5. Hypothetical “modes” of processing that do or do not rely on the phase of neural oscillations during*
456 *selective (A) and divided attention (B). A) If the timing of relevant events is unknown, the auditory system might*
457 *need to suppress neural oscillations to avoid a loss of information at the low-excitability phase, and operate in a*
458 *mode of continuous high excitability (continuous purple line), whereas the visual system can operate rhythmically*
459 *(dashed purple), due to its slower sensory dynamics. If events become irrelevant, the auditory system might change*
460 *to a mode of periodic high sensitivity, reflected in a rhythmic sampling of irrelevant information (continuous*
461 *yellow). The visual system might not need these high-sensitivity moments for irrelevant information, resulting in a*
462 *continuous mode of low excitability (dashed yellow). B) Three hypothetical modes of processing during auditory*
463 *divided attention. When multiple targets need to be processed, the auditory system might operate in a continuous*
464 *mode of processing to avoid loss of information at a low-excitability phase (I, left). Such a mode would lead to a*
465 *detection of these targets that is independent of phase (I, right). Alternatively, the presence of multiple targets might*
466 *require an alternation of attentional focus between possible sound frequencies that relies on neural phase at the*
467 *frequency f . This might be achieved by prioritizing different sound frequencies at different neural phases (II, left),*
468 *leading to a target detection probability that depends on the phase at f , and a preferred phase for detection that*
469 *changes with sound frequency of the target (II, right). In an alternative rhythmic mode, possible sound frequencies*
470 *are processed at the same (high-excitability) phase of f , but in subsecutive cycles (III, left), leading to a phase effect*
471 *at $f/2$ and to similar preferred phases across sound frequencies (III, right). The latter is what we have observed in the*
472 *current study (cf. Figure 4A).*

473

474 **Alpha and theta oscillations modulate distinct processing steps of irrelevant events**

475 We found that the pre-stimulus phase of alpha oscillations predicts a relatively early response to
476 task-irrelevant tones whereas the pre-stimulus phase of theta oscillations predicts later responses
477 (Figure 3). We speculate that this finding can be attributed to distinct steps in the processing of
478 task-irrelevant events that depend on different oscillatory frequency bands.

479 The phase of alpha oscillations is posited to gate perception via pulsed inhibition (Jensen
480 & Mazaheri, 2010) at early stages of cortical processing where the encoding of sensory events
481 takes place (Klimesch et al., 2011). Indeed, the phasic modulation of the early evoked response
482 in the alpha band seemed to originate from relatively early stages of the auditory cortical
483 hierarchy in our study (Figure 3B). The timing of the early evoked GFP (~119 ms) is well in line
484 with components of stimulus-evoked neural responses (e.g., P1, N1) that have been associated
485 with stimulus encoding (Näätänen & Picton, 1987). Although imaging methods with higher
486 spatial localisation are required to validate this hypothesis, we speculate that alpha oscillations
487 phasically modulate the encoding of task-irrelevant events (e.g., distractors).

488 Stimulus-evoked neural responses at later delays have been associated with higher-level
489 cognitive operations, such as distractibility (Chao & Knight, 1995) as well as response execution
490 and inhibition (Bokura et al., 2001). Theta oscillations in the frontal cortex have been considered
491 a neural proxy of executive control (Mizuhara & Yamaguchi, 2007; Sauseng et al., 2007). A
492 previous study showed evidence for a theta rhythm in distractibility by showing that perceptual
493 sensitivity is explained by pre-distractor theta phase (Lui et al., 2023). It is thus possible that the
494 propensity to ignore task-irrelevant events depends on pre-stimulus theta oscillations. The later
495 timing of the theta-phase modulation in our study as well as its localisation to more frontal brain
496 regions is in line with this assumption (Figure 3D). This effect may therefore reflect the
497 inhibition of the processing of task-irrelevant events that occurs after their encoding. The fact
498 that only early phasic effects were present, but the later theta-phase modulation was absent
499 during divided attention (Figure 4) further supports this assumption, as no distractors needed to
500 be inhibited in that condition.

501 It remains an open question why the strongest phase effect occurred relatively early
502 before tone onset (~-800 to -600 ms), and earlier than what has previously been reported (Busch
503 & VanRullen, 2010; Harris et al., 2018; Zazio et al., 2021). On the one hand, the closer to
504 stimulus onset, the stronger is the “contamination” of phase estimates by post-stimulus data
505 (Vinao-Carl et al., 2024; Zoefel & Heil, 2013), potentially obscuring maxima closer to tone
506 onset. On the other hand, the earliest time points that remain unaffected by temporal smearing
507 can be estimated precisely and do not show the strongest effects (Figures 2 – 4). Other factors
508 might therefore play a role and need to be identified in future work. For example, it is possible
509 that the perception and suppression of task-irrelevant auditory events is achieved through
510 connectivity with other brain regions that eventually cascades down to the auditory system at
511 stimulus onset.

512

513 **A rhythmic mode in auditory divided attention**

514 We found evidence for a rhythmic mode of processing during auditory divided attention, and our
515 results provide insights into a mechanistic implementation of such a mode. The phasic
516 modulation of the early GFP evoked by the two tones (Figure 4A) contradicts our initial
517 hypothesis that neural oscillations are suppressed during divided attention to task-relevant tones
518 (Figure 5B-I). Nevertheless, the two tones (low- and high sound frequency) could be processed
519 in the same oscillatory cycle but at different phases (Figure 5B-II) as often proposed in the
520 context of neural oscillations (Gips et al., 2016; Jensen et al., 2014), or in subsecutive cycles
521 (Gaillard & Ben Hamed, 2022) and at a similar phase (Figure 5B-III). Based on predicted results
522 patterns that can distinguish these alternatives (Figure 5B, right panels), our results favour the
523 second one, as (1) the frequency of the early modulation is divided approximately by two as
524 compared to the processing of a single tone (compare Figure 3A and 4A); and (2) phases do not
525 differ between the low and high frequency tones (Figure 4B,C). Therefore, our results suggest
526 that alpha oscillations do not only modulate the processing of task-irrelevant information, but
527 also the early stages of task-relevant processing during divided attention, alternating between
528 possible sound frequencies of targets.

529 This conclusion is well in line with previous research. For instance, the frequency of visual
530 perception decreases with increasing number of to-be-attended features (Holcombe & Chen,
531 2013; Schmid et al., 2022). The spotlight of attention has been posited to alternate between two
532 locations when both are attended, dividing an overall ~8 Hz rhythm into a ~4 Hz fluctuation in
533 perceptual sensitivity per location (Landau & Fries, 2012; Song et al., 2014; Zoefel & Sokoliuk,
534 2014). In the auditory modality, a similar alternation between the two ears has been reported
535 during divided attention (Ho et al., 2017). We here extend this mechanism to an alternation
536 between sound frequencies, supporting the previous observation that oscillatory mechanisms
537 follow the tonotopic organisation of the auditory cortex (Lakatos et al., 2013; L’Hermite &
538 Zoefel, 2023).

539

540 Conclusion

541 By showing that the processing of task-irrelevant but not task-relevant tones depends on
542 the pre-stimulus phase of neural oscillations during selective attention, we here provide evidence
543 that oscillatory mechanisms in audition critically depend on the degree of possible information
544 loss. We propose that this effect represents a crucial difference to the visual modality which
545 might not be equally responsive to sensory information (Figure 5). During divided attention,
546 cycles of alpha oscillations seem to alternate between possible targets similar to what was
547 observed in vision, suggesting an attentional process that generalises across modalities.

548

549

References

550 Berens, P. (2009). CircStat: A MATLAB Toolbox for Circular Statistics. *Journal of Statistical Software*,
551 31, 1–21. <https://doi.org/10.18637/jss.v031.i10>

552 Berti, S., & Schröger, E. (2001). A comparison of auditory and visual distraction effects: Behavioral and
553 event-related indices. *Cognitive Brain Research*, 10(3), 265–273. <https://doi.org/10.1016/S0926->
554 6410(00)00044-6

555 Bokura, H., Yamaguchi, S., & Kobayashi, S. (2001). Electrophysiological correlates for response
556 inhibition in a Go/NoGo task. *Clinical Neurophysiology*, 112(12), 2224–2232.
557 [https://doi.org/10.1016/S1388-2457\(01\)00691-5](https://doi.org/10.1016/S1388-2457(01)00691-5)

558 Brainard, D. H. (1997). The psychophysics toolbox. *Spatial Vision*, 10(4), 433–436.
559 <https://doi.org/10.1163/156856897X00357>

560 Busch, N. A., Dubois, J., & VanRullen, R. (2009). The Phase of Ongoing EEG Oscillations Predicts
561 Visual Perception. *Journal of Neuroscience*, 29(24), 7869–7876.
562 <https://doi.org/10.1523/JNEUROSCI.0113-09.2009>

563 Busch, N. A., & VanRullen, R. (2010). Spontaneous EEG oscillations reveal periodic sampling of visual
564 attention. *Proceedings of the National Academy of Sciences*, 107(37), 16048–16053.
565 <https://doi.org/10.1073/pnas.1004801107>

566 Chao, L. L., & Knight, R. T. (1995). Human prefrontal lesions increase distractibility to irrelevant sensory
567 inputs. *Neuroreport: An International Journal for the Rapid Communication of Research in*
568 *Neuroscience*, 6(12), 1605–1610. <https://doi.org/10.1097/00001756-199508000-00005>

569 Dugué, L., Marque, P., & VanRullen, R. (2011). The Phase of Ongoing Oscillations Mediates the Causal
570 Relation between Brain Excitation and Visual Perception. *The Journal of Neuroscience*, 31(33), 11889–
571 11893. <https://doi.org/10.1523/JNEUROSCI.1161-11.2011>

572 Dugué, L., Marque, P., & VanRullen, R. (2015). Theta Oscillations Modulate Attentional Search
573 Performance Periodically. *Journal of Cognitive Neuroscience*, 27(5), 945–958.
574 https://doi.org/10.1162/jocn_a_00755

575 Fiebelkorn, I. C., Saalmann, Y. B., & Kastner, S. (2013). Rhythmic sampling within and between objects
576 despite sustained attention at a cued location. *Current Biology*, 23(24), 2553–2558.
577 <https://doi.org/10.1016/j.cub.2013.10.063>

578 Gaillard, C., & Ben Hamed, S. (2022). The neural bases of spatial attention and perceptual rhythms.
579 *European Journal of Neuroscience*, 55(11–12), 3209–3223. <https://doi.org/10.1111/ejn.15044>

580 Gips, B., van der Eerden, J. P. J. M., & Jensen, O. (2016). A biologically plausible mechanism for
581 neuronal coding organized by the phase of alpha oscillations. *European Journal of Neuroscience*, 44(4),
582 2147–2161. <https://doi.org/10.1111/ejn.13318>

583 Harris, A. M., Dux, P. E., & Mattingley, J. B. (2018). Detecting unattended stimuli depends on the phase
584 of prestimulus neural oscillations. *The Journal of Neuroscience*, 38(12), 3092–3101.
585 <https://doi.org/10.1523/JNEUROSCI.3006-17.2018>

586 Helfrich, R. F., Fiebelkorn, I. C., Szczepanski, S. M., Lin, J. J., Parvizi, J., Knight, R. T., & Kastner, S.
587 (2018). Neural mechanisms of sustained attention are rhythmic. *Neuron*, 99(4), 854-865.e5.
588 <https://doi.org/10.1016/j.neuron.2018.07.032>

589 Henry, M. J., & Obleser, J. (2012). Frequency modulation entrains slow neural oscillations and optimizes
590 human listening behavior. *Proceedings of the National Academy of Sciences*, 109(49), 20095–20100.

591 Ho, H. T., Leung, J., Burr, D. C., Alais, D., & Morrone, M. C. (2017). Auditory sensitivity and decision
592 criteria oscillate at different frequencies separately for the two ears. *Current Biology*, 27(23), 3643-
593 3649.e3. <https://doi.org/10.1016/j.cub.2017.10.017>

594 Holcombe, A. O., & Chen, W.-Y. (2013). Splitting attention reduces temporal resolution from 7 Hz for
595 tracking one object to <3 Hz when tracking three. *Journal of Vision*, 13(1), 12.
596 <https://doi.org/10.1167/13.1.12>

597 Jensen, O., Gips, B., Bergmann, T. O., & Bonnefond, M. (2014). Temporal coding organized by coupled
598 alpha and gamma oscillations prioritize visual processing. *Trends in Neurosciences*, 37(7), 357–369.
599 <https://doi.org/10.1016/j.tins.2014.04.001>

600 Jensen, O., & Mazaheri, A. (2010). Shaping Functional Architecture by Oscillatory Alpha Activity:
601 Gating by Inhibition. *Frontiers in Human Neuroscience*, 4. <https://doi.org/10.3389/fnhum.2010.00186>

602 Klimesch, W., Fellinger, R., & Freunberger, R. (2011). Alpha Oscillations and Early Stages of Visual
603 Encoding. *Frontiers in Psychology*, 2. <https://doi.org/10.3389/fpsyg.2011.00118>

604 Kubovy, M. (1988). Should we resist the seductiveness of the space: Time: Vision: Audition analogy?
605 *Journal of Experimental Psychology: Human Perception and Performance*, 14(2), 318–320.
606 <https://doi.org/10.1037/0096-1523.14.2.318>

607 Lakatos, P., Gross, J., & Thut, G. (2019). A new unifying account of the roles of neuronal entrainment.
608 *Current Biology*, 29(18), R890–R905. <https://doi.org/10.1016/j.cub.2019.07.075>

609 Lakatos, P., Karmos, G., Mehta, A. D., Ulbert, I., & Schroeder, C. E. (2008). Entrainment of neuronal
610 oscillations as a mechanism of attentional selection. *Science*, 320(5872), 110–113.
611 <https://doi.org/10.1126/science.1154735>

612 Lakatos, P., Musacchia, G., O'Connel, M. N., Falchier, A. Y., Javitt, D. C., & Schroeder, C. E. (2013).
613 The spectrotemporal filter mechanism of auditory selective attention. *Neuron*, 77(4), 750–761.
614 <https://doi.org/10.1016/j.neuron.2012.11.034>

615 Landau, A. N., & Fries, P. (2012). Attention samples stimuli rhythmically. *Current Biology*, 22(11),
616 1000–1004. <https://doi.org/10.1016/j.cub.2012.03.054>

617 L'Hermite, S., & Zoefel, B. (2023). Rhythmic Entrainment Echoes in Auditory Perception. *Journal of
618 Neuroscience*, 43(39), 6667–6678. <https://doi.org/10.1523/JNEUROSCI.0051-23.2023>

619 Lui, T. K.-Y., Obleser, J., & Wöstmann, M. (2023). Slow neural oscillations explain temporal fluctuations
620 in distractibility. *Progress in Neurobiology*, 226, 102458.
621 <https://doi.org/10.1016/j.pneurobio.2023.102458>

622 Lui, T. K.-Y., & Wöstmann, M. (2022). Effects of temporally regular versus irregular distractors on goal-
623 directed cognition and behavior. *Scientific Reports*, 12, 10020. [https://doi.org/10.1038/s41598-022-13211-3](https://doi.org/10.1038/s41598-022-
624 13211-3)

625 Mathewson, K. E., Gratton, G., Fabiani, M., Beck, D. M., & Ro, T. (2009). To See or Not to See:
626 Prestimulus Phase Predicts Visual Awareness. *Journal of Neuroscience*, 29(9), 2725–2732.
627 <https://doi.org/10.1523/JNEUROSCI.3963-08.2009>

628 Mizuhara, H., & Yamaguchi, Y. (2007). Human cortical circuits for central executive function emerge by
629 theta phase synchronization. *NeuroImage*, 36(1), 232–244.
630 <https://doi.org/10.1016/j.neuroimage.2007.02.026>

631 Näätänen, R., & Picton, T. (1987). The N1 Wave of the Human Electric and Magnetic Response to
632 Sound: A Review and an Analysis of the Component Structure. *Psychophysiology*, 24(4), 375–425.
633 <https://doi.org/10.1111/j.1469-8986.1987.tb00311.x>

634 Obleser, J., & Kayser, C. (2019). Neural entrainment and attentional selection in the listening brain.
635 *Trends in Cognitive Sciences*, 23(11), 913–926. <https://doi.org/10.1016/j.tics.2019.08.004>

636 Oostenveld, R., Fries, P., Maris, E., & Schoffelen, J.-M. (2011). FieldTrip: Open source software for
637 advanced analysis of MEG, EEG, and invasive electrophysiological data. *Computational Intelligence and*
638 *Neuroscience*, 2011, 156869. <https://doi.org/10.1155/2011/156869>

639 Pachitariu, M., Lyamzin, D. R., Sahani, M., & Lesica, N. A. (2015). State-Dependent Population Coding
640 in Primary Auditory Cortex. *The Journal of Neuroscience*, 35(5), 2058–2073.
641 <https://doi.org/10.1523/JNEUROSCI.3318-14.2015>

642 Prins, N., & Kingdom, F. A. A. (2018). Applying the model-comparison approach to test specific research
643 hypotheses in psychophysical research using the palamedes toolbox. *Frontiers in Psychology*, 9, 1250.
644 <https://doi.org/10.3389/fpsyg.2018.01250>

645 Sauseng, P., Hoppe, J., Klimesch, W., Gerloff, C., & Hummel, F. C. (2007). Dissociation of sustained
646 attention from central executive functions: Local activity and interregional connectivity in the theta range.
647 *European Journal of Neuroscience*, 25(2), 587–593. <https://doi.org/10.1111/j.1460-9568.2006.05286.x>

648 Schmid, R. R., Pomper, U., & Ansorge, U. (2022). Cyclic reactivation of distinct feature dimensions in
649 human visual working memory. *Acta Psychologica*, 226, 103561.
650 <https://doi.org/10.1016/j.actpsy.2022.103561>

651 Schroeder, C. E., & Lakatos, P. (2009). Low-frequency neuronal oscillations as instruments of sensory
652 selection. *Trends in Neurosciences*, 32(1), 9–18. <https://doi.org/10.1016/j.tins.2008.09.012>

653 Song, K., Meng, M., Chen, L., Zhou, K., & Luo, H. (2014). Behavioral Oscillations in Attention:
654 Rhythmic α Pulses Mediated through θ Band. *Journal of Neuroscience*, 34(14), 4837–4844.
655 <https://doi.org/10.1523/JNEUROSCI.4856-13.2014>

656 van Bree, S., Sohoglu, E., Davis, M. H., & Zoefel, B. (2021). Sustained neural rhythms reveal
657 endogenous oscillations supporting speech perception. *PLOS Biology*, 19(2), e3001142.
658 <https://doi.org/10.1371/journal.pbio.3001142>

659 Van Veen, B. D., Van Drongelen, W., Yuchtman, M., & Suzuki, A. (1997). Localization of brain
660 electrical activity via linearly constrained minimum variance spatial filtering. *IEEE Transactions on*
661 *Biomedical Engineering*, 44(9), 867–880. <https://doi.org/10.1109/10.623056>

662 VanRullen, R. (2016a). How to Evaluate Phase Differences between Trial Groups in Ongoing
663 Electrophysiological Signals. *Frontiers in Neuroscience*, 10. <https://doi.org/10.3389/fnins.2016.00426>

664 VanRullen, R. (2016b). Perceptual Cycles. *Trends in Cognitive Sciences*, 20(10), 723–735.
665 <https://doi.org/10.1016/j.tics.2016.07.006>

666 VanRullen, R., Zoefel, B., & Ilhan, B. (2014). On the cyclic nature of perception in vision versus
667 audition. *Philosophical Transactions of the Royal Society B: Biological Sciences*, 369(1641), 20130214.
668 <https://doi.org/10.1098/rstb.2013.0214>

669 Vinao-Carl, M., Gal-Shohet, Y., Rhodes, E., Li, J., Hampshire, A., Sharp, D., & Grossman, N. (2024).
670 Just a phase? Causal probing reveals spurious phasic dependence of sustained attention. *NeuroImage*,
671 285, 120477. <https://doi.org/10.1016/j.neuroimage.2023.120477>

672 Wöstmann, M., Lui, T. K.-Y., Fries, K. H., Kreitewolf, J., Naujokat, M., & Obleser, J. (2020). The
673 vulnerability of working memory to distraction is rhythmic. *Neuropsychologia*, 146, 107505.
674 <https://doi.org/10.1016/j.neuropsychologia.2020.107505>

675 Zazio, A., Ruhnau, P., Weisz, N., & Wutz, A. (2021). Pre-stimulus alpha-band power and phase
676 fluctuations originate from different neural sources and exert distinct impact on stimulus-evoked
677 responses. *European Journal of Neuroscience*, ejn.15138. <https://doi.org/10.1111/ejn.15138>

678 Zoefel, B., Davis, M. H., Valente, G., & Riecke, L. (2019). How to test for phasic modulation of neural
679 and behavioural responses. *NeuroImage*, 202, 116175. <https://doi.org/10.1016/j.neuroimage.2019.116175>

680 Zoefel, B., & Heil, P. (2013). Detection of near-threshold sounds is independent of EEG phase in
681 common frequency bands. *Frontiers in Psychology*, 4. <https://doi.org/10.3389/fpsyg.2013.00262>

682 Zoefel, B., & Sokoliuk, R. (2014). Investigating the Rhythm of Attention on a Fine-Grained Scale:
683 Evidence from Reaction Times. *Journal of Neuroscience*, 34(38), 12619–12621.
684 <https://doi.org/10.1523/JNEUROSCI.2134-14.2014>

685 Zoefel, B., & VanRullen, R. (2017). Oscillatory mechanisms of stimulus processing and selection in the
686 visual and auditory systems: State-of-the-art, speculations and suggestions. *Frontiers in Neuroscience*, 11,
687 13.

688